W. T. Chen
C. W. Nelson

Thermal Stress in Bonded Joints

This paper considers the stress distributions in bonded materials induced by differential expansion or contraction of these materials. The analytical approach is similar to the lap joint theories attributed to Volkersen and expanded by Goland and Reissner. Several simple and typical analytical models are presented to bring out the relative importance of different geometrical and material parameters and to give some insight into different modes in which the bonds might fail.

Introduction

The reliability of any electronic device depends to a great extent on its construction. The structural design and fabrication dictate the amount of power dissipation, the number of thermal cycles, and the intensity of mechanical impact and vibration which the device can sustain without degrading its performance.

Since electronic devices are characterized by heterogeneous materials joined together by different methods, including adhesives and solder, a key consideration in the packaging of the devices is that the bonds between the different materials are capable of sustaining the mechanical and thermal stresses over the service life of the device. A general discussion of the commonly used materials and their fabrication and assembly processes may be found in [1].

The reliability of electronic devices and their packaging considerations are discussed in many technical journals and monographs. Some recent review papers are found in [2]. This paper considers the stresses induced in bonded materials by differential expansion or contraction of these materials. A number of simplifying assumptions made in the present treatment are described later in this paper. These are believed to be good approximations leading to valid results provided that the elastic modulus of the adherend is about ten (or more) times that of the adhesive and provided that the thickness ratio of adherend to adhesive also is about ten (or more). The guiding philosophy behind this paper is to keep the treatment simple. Then, any or all parameters can be varied through a reasonable range easily, and considerable insight can be obtained as to the effects of various physical parameters on the thermal stresses.

This paper presents several simple and typical analytical models to bring out the relative importance of different geometrical and material parameters. It also gives some insight into different modes in which the bonds might fail.

While one usually associates thermal stress with the stresses that arise from high temperature service conditions on heterogeneous materials with dissimilar thermal expansion coefficients, such stresses can also be introduced during the fabrication processes. One such example is the internal stress condition produced in the silicon oxide film during the etching, diffusion, and metallization processes. Many films show "intrinsic" stresses which greatly exceed the calculated values for thermal stresses [3].

Taylor and Yuan [4] studied fracture failure in some semiconductor devices, and developed mathematical analysis for thermal stress concentrations in the silicon bond area to explain the observed fracture. The analytical approach adopted by Taylor and Yuan has its roots in the lap joint theory commonly attributed to Volkersen [5].

Copyright 1979 by International Business Machines Corporation. Copying is permitted without payment of royalty provided that (1) each reproduction is done without alteration and (2) the *Journal* reference and IBM copyright notice are included on the first page. The title and abstract may be used without further permission in computer-based and other information-service systems. Permission to *republish* other excerpts should be obtained from the Editor.

In that theory the joint (adhesive, solder) was treated as a distribution of shear springs similar to the well-known Winkler foundation theory. The joined materials (adherends) were treated as beams in tension. The Volkersen lap joint theory has been further expanded and improved in the now classic paper by Goland and Reissner [6]. With the widespread use of adhesives today, it is not surprising that many of the later developments are motivated by calculation of stress in adhesive bonds. Fortunately, the mathematical analyses are usually applicable to other bond materials, given the assumption that the joint material (adhesive) is less stiff than the joined materials (adherend).

Further development of the adhesive joint analysis may be found in the survey articles by Benson [7] and in many monographs [8–12]. There have been many publications on the subject since the work of Goland and Reissner, and an exhaustive bibliography would be outside the scope of this paper. Some recent contributions may be found in [13, 14]. The present paper expands from the work of Taylor and Yuan to other physical conditions and geometries.

Process engineers and adhesive scientists often employ peel tests to assess the strength of the bond. To relate the measured peel force to the maximum stresses in the peeling process, the peel adhesion theories developed by Spies [15], Bikerman [16, 17], and Kaelble [18, 19] are used. These theories are also founded upon the Winkler type foundation theory for the joint material. Sometimes a peel test may be used for obtaining a bond strength to be used as a criterion of failure in the thermal stress calculations of the present paper. However, if this is done, care should be taken to ensure that the basic assumptions used in the theory for obtaining bond strength from a measured peel force are compatible with the assumptions used for computing the bond stress in the actual device by the methods of this paper.

The first case considered in this paper is three elastic layers bonded together at two interfaces. The layers are assumed to remain straight as in Volkersen's theory. The two-layer elastic solution is also given and is found to reduce to Taylor and Yuan's result when one layer is assumed to be rigid. The analyses for circular plates bonded together are also studied.

It is shown that in the limit of radius-to-thickness ratio approaching infinity, the previous solution can be recovered. Finally, the two elastic layers are allowed to bend freely, such as in flexible printed circuits. It is shown that the analysis follows naturally from Goland and Reissner's work. It is particularly interesting to find that stress concentration in shear and tension occurs simultaneously, and debonding would be mixed mode in character.

Analysis

Three elastic layers with two bonded joints (adhesive, solder)

The assumptions inherent in the Volkerson's lap joint analysis are adopted here with the addition of thermal consideration. The three layers being bonded together are assumed to be of uniform thicknesses (t_1, t_2, t_3) and with elastic moduli (E_1, E_2, E_3), and thermal expansion coefficients (α_1, α_2, α_3). The joint between layers 1 and 2 will have thickness η and shear modulus G. The joint between layers 1 and 3 will have thickness η' and shear modulus G'.

As shown in Fig. 1, the forces in the elastic layers are assumed to be uniform through the thickness (F_1, F_2, F_3). The bonded joints exert shear stress τ between layers 1 and 2, and shear stress τ' between layers 1 and 3.

At some temperature T_0 the joints are stress free. What will be the shear stresses τ and τ' and forces F_1, F_2, F_3 with a temperature change of T?

Considering the equilibrium of forces in the x direction (see Fig. 1), the following three equations are derived:

$$\frac{dF_1}{dx} + \tau' - \tau = 0,$$

$$\frac{dF_2}{dx} + \tau = 0,$$

$$\frac{dF_3}{dx} - \tau' = 0. \tag{1}$$

The stress-strain-temperature equations of the three layers are

$$\frac{du_1}{dx} = \frac{F_1}{E_1 t_1} + \alpha_1 T,$$

$$\frac{du_2}{dx} = \frac{F_2}{E_2 t_2} + \alpha_2 T,$$

$$\frac{du_3}{dx} = \frac{F_3}{E_3 t_3} + \alpha_3 T. \tag{2}$$

And for the bonded joint materials under shear, the stress-strain relationships are

$$\frac{\tau}{G} = \frac{u_1 - u_2}{\eta},$$

$$\frac{\tau'}{G'} = \frac{u_3 - u_1}{\eta'}. \tag{3}$$

The solutions of the previous set of eight equations are straightforward. The general solution for τ and τ' is found to be

$$\tau = A_1 \sinh \beta_1 x + A_2 \sinh \beta_2 x + A_3 \cosh \beta_1 x + A_4 \cosh \beta_2 x,$$

$$\tau' = A_1 k_1 \sinh \beta_1 x + A_2 k_2 \sinh \beta_2 x + A_3 k_3 \cosh \beta_1 x + A_4 k_4 \cosh \beta_2 x. \tag{4}$$

Here $\pm\beta_1$ and $\pm\beta_2$ are roots of the equation

$$\beta^4 - \frac{1}{E_1 t_1}\left[\frac{G}{\eta}\left(1 + \frac{E_1 t_1}{E_2 t_2}\right) + \frac{G'}{\eta'}\left(1 + \frac{E_1 t_1}{E_3 t_3}\right)\right]\beta^2 + \frac{GG'}{(E_1 t_1)^2 \eta\eta'}\left[\left(1 + \frac{E_1 t_1}{E_2 t_2}\right)\left(1 + \frac{E_1 t_1}{E_3 t_3}\right) - 1\right] = 0, \tag{5}$$

and the constants A_i, k_i $(i = 1, 4)$ are to be determined by boundary conditions. Let us impose the boundary conditions that the bond areas are completely filled up as in Fig. 1, and that the ends $x = \pm\ell$ are free. Four of the constants are found to be zero:

$$A_3 = A_4 = K_3 = K_4 = 0.$$

Write the shear stresses as

$$\tau = C_1 \frac{\sinh \beta_1 x}{\cosh \beta_1 \ell} + C_2 \frac{\sinh \beta_2 x}{\cosh \beta_2 \ell}, \tag{6}$$

$$\tau' = C_1 k_1 \frac{\sinh \beta_1 x}{\cosh \beta_1 \ell} + C_2 k_2 \frac{\sinh \beta_2 x}{\cosh \beta_2 \ell}, \tag{7}$$

$$k_i = E_1 t_1 \left[\left(\frac{1}{E_1 t_1} + \frac{1}{E_2 t_2}\right) - \frac{\beta_i^2 \eta}{G}\right], \tag{8}$$

$$C_1 = \frac{G\beta_1[D_2 k_2 + D_3]}{E_1 t_1 \eta(\beta_1^2 - \beta_2^2)}, \tag{9A}$$

$$C_2 = \frac{G\beta_2[D_2 k_1 + D_3]}{E_1 t_1 \eta(\beta_2^2 - \beta_1^2)}, \tag{9B}$$

and D_1, D_2, D_3 are constants defined by

$$D_1 = \frac{E_1 t_1[E_3 t_3(\alpha_3 - \alpha_1) + E_2 t_2(\alpha_2 - \alpha_1)]T}{E_1 t_1 + E_2 t_2 + E_3 t_3},$$

$$D_2 = \frac{E_2 t_2[E_1 t_1(\alpha_1 - \alpha_2) + E_3 t_3(\alpha_3 - \alpha_2)]T}{E_1 t_1 + E_2 t_2 + E_3 t_3},$$

$$D_3 = \frac{E_3 t_3[E_1 t_1(\alpha_1 - \alpha_3) + E_2 t_2(\alpha_2 - \alpha_3)]T}{E_1 t_1 + E_2 t_2 + E_3 t_3}. \tag{10}$$

It is clear, merely from the general form of the equations (6) and (7), that the shear stresses τ and τ' vary from zero at the middle symmetric point to a maximum at the edge $x = \ell$. When the layer's length-to-joint thickness ratio is very large, the stresses at the edge approach

$$\tau(x = \ell) = C_1 + C_2,$$

$$\tau'(x = \ell) = C_1 k_1 + C_2 k_2. \tag{11}$$

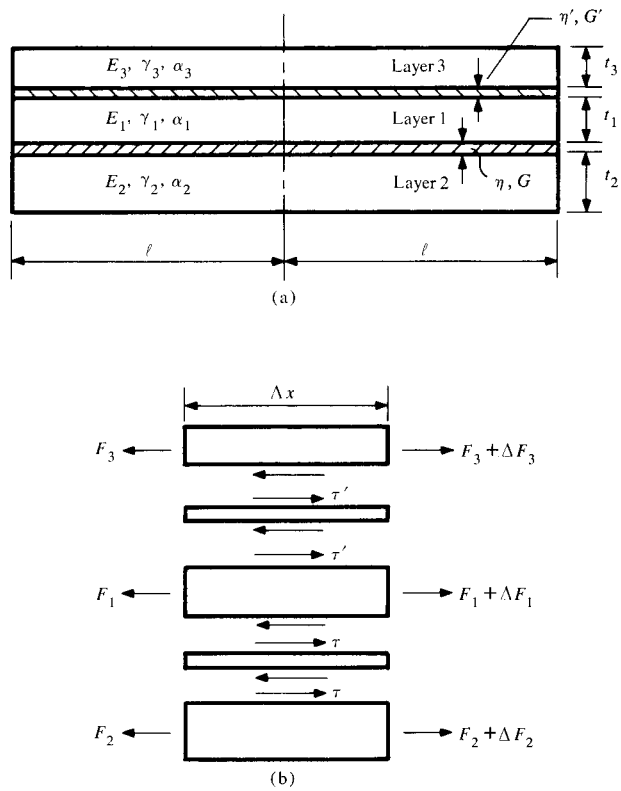

Figure 1 (a) Notations on three joined layers. (b) Force balance on three joined layers for a section dx.

These are the expressions for the maximum shear stresses at the edge of the two bonded joints. Discussion of numerical examples will be reserved for a later section.

Two elastic layers joined by one bonded joint

The analysis follows the same steps as before. In the case of a completely filled joint, the shear stress is given by

$$\tau = \frac{(\alpha_1 - \alpha_2)TG \sinh \beta x}{\beta\eta \cosh \beta\ell}, \tag{12}$$

where

$$\beta^2 = \frac{G}{\eta}\left(\frac{1}{E_1 t_1} + \frac{1}{E_2 t_2}\right). \tag{13}$$

Physically the shear stress is zero at the center, and increases gradually to a maximum at the free edge. The value of this maximum stress is

$$\tau_{\max} = \frac{(\alpha_1 - \alpha_2)TG \tanh \beta\ell}{\beta\eta}. \tag{14}$$

Often it may be sufficient to take $\tanh \beta\ell \sim 1$ and use the estimate

$$\tau_{\max} = \frac{(\alpha_1 - \alpha_2)TG}{\beta\eta}. \tag{15}$$

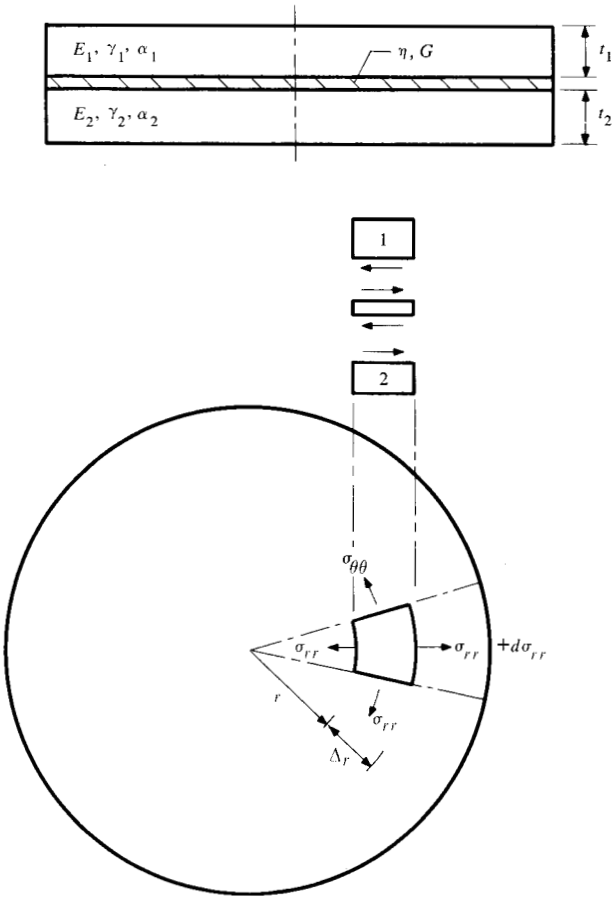

Figure 2 Two circular sheets bonded together.

If $\beta\ell$ could be small, then the shear stress would approach the usual simplified estimate of

$$\tau = \frac{(\alpha_1 - \alpha_2)T\ell G}{\eta}, \tag{16}$$

since $(\tanh \beta\ell)/\beta\ell$ would approach unity. However, with physically realistic parameter, $\beta\ell$ is never small. Therefore the usual simplified estimate [Eq. (16)] is often a poor approximation.

Two circular sheets bonded together

The foregoing analysis has been one-dimensional. It was considered useful to study the axisymmetric situation of two circular sheets bonded together as shown in Fig. 2. The analytical development is given in Appendix A. As may be expected the solution is in the form of modified Bessel functions. In the case where the bond area between the two sheets is completely filled, the shear stress is zero at the center of the circle, and gradually rises to the free edge with increasing r according to the formula

$$\tau = \frac{2(\alpha_1 - \alpha_2)TG}{\eta\beta(C_1 + C_2)} I_1(\beta r), \tag{17}$$

$$\beta^2 = \frac{G}{\eta}\left(\frac{1 - \gamma_1^2}{E_1 t_1} + \frac{1 - \gamma_2^2}{E_2 t_2}\right), \tag{18}$$

$$C_1 = -\frac{2}{1 + \gamma_1}\left[\frac{1 - \gamma_1}{\beta R} I_1(\beta R) - I_0(\beta R)\right], \tag{19A}$$

$$C_2 = -\frac{2}{1 + \gamma_2}\left[\frac{1 - \gamma_2}{\beta R} I_1(\beta R) - I_0(\beta R)\right]. \tag{19B}$$

The maximum stress occurs at $r = R$, and is equal to

$$\tau_{\max} = \frac{TG(\alpha_1 - \alpha_2)}{\eta\beta}\left\{\frac{1}{1 + \gamma_1}\left[\frac{1 - \gamma_1}{\beta R} - \frac{I_0(\beta R)}{I_1(\beta R)}\right] + \frac{1}{1 + \gamma_2}\left[\frac{1 - \gamma_2}{\beta R} - \frac{I_0(\beta R)}{I_1(\beta R)}\right]\right\}. \tag{20}$$

Two elastic layers with one joint allowing free flexure

When two layers expand unequally, but are bonded together, there is the natural tendency for the composite to bend. This is the basic theory behind a bimetallic thermostat analyzed by S. Timoshenko [20] many years ago. Timoshenko assumed that the two layers behave like beams capable of axial and bending deformations, and that there is no slip at the interface between the two layers. In this section we consider that the two layers are separated by an amount η and are filled with a material capable of deforming under shear and tension. This is essentially the approach taken by Goland and Reissner [6], who dealt with externally applied forces rather than the internally generated thermal stress.

Figure 3 shows the forces and moments acting on an elementary section of the bonded composite. Equilibrium of moments requires that

$$\frac{dM_1}{dx} - V_1 + \tau_0 \frac{t_1}{2} = 0,$$

$$\frac{dM_2}{dx} - V_2 + \tau_0 \frac{t_2}{2} = 0. \tag{21}$$

Equilibrium of horizontal forces requires that

$$\frac{dF_1}{dx} - \tau_0 = 0,$$

$$\frac{dF_2}{dx} + \tau_0 = 0. \tag{22}$$

And for equilibrium of vertical forces

$$\frac{dV_1}{dx} - \sigma_0 = 0,$$

$$\frac{dV_2}{dx} + \sigma_0 = 0. \tag{23}$$

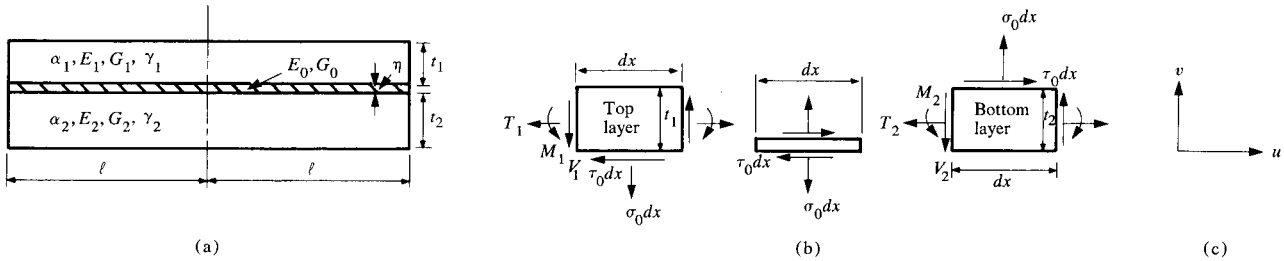

Figure 3 (a) Notations on joined layers. (b) Force and moment diagrams on a section dx. (c) Positive sense of displacement components.

The next step is to relate moments and forces to displacements. From elementary bending theories,

$$\frac{d^2v_1}{dx^2} = -\frac{M_1}{D_1}, \quad \frac{d^2v_2}{dx^2} = -\frac{M_2}{D_2}, \tag{24}$$

where

$$D_i = \frac{E_i t_i^3}{12(1-\gamma_i^2)}, \tag{25}$$

and

$$\frac{du_1}{dx} = \frac{(1-\gamma_1^2)F_1}{E_1 t_1} - \frac{6(1-\gamma_1^2)M}{E_1 t_1^2} + (1+\gamma_1)\alpha_1 T, \tag{26}$$

$$\frac{du_2}{dx} = \frac{(1-\gamma_2^2)F_2}{E_2 t_2} + \frac{6(1-\gamma_2^2)M_2}{E_2 t_2^2} + (1+\gamma_2)\alpha_2 T. \tag{27}$$

Finally, the stress in the joint material is assumed to depend on the displacements (u_1, v_1) and (u_2, v_2), according to the equations

$$\frac{\tau_0}{G_0} = \frac{u_1 - u_2}{\eta}, \tag{28}$$

$$\frac{\sigma_0}{E_0} = \frac{v_1 - v_2}{\eta}. \tag{29}$$

Here G_0 and E_0 are shear modulus and Young's modulus of the joint material.

Now the stress analysis problem is fully formulated. With the appropriate boundary conditions, the analysis is complete. An inventory of Eqs. (21) to (29) discloses that there are twelve such equations. The above set of equations can be reduced to a single sixth-order differential equation for σ_0. A solution of the differential equation can be found containing six constants of integration permitting the six boundary conditions to be satisfied. This sixth-order differential equation is

$$\frac{d^6\sigma_0}{dx^6} - \frac{G_0 c}{\eta}\frac{d^4\sigma_0}{dx^4} + \frac{E_0 b}{\eta}\frac{d^2\sigma_0}{dx^2} - \frac{G_0 E_0 (bc - a^2)\sigma_0}{\eta^2} = 0, \tag{30}$$

where the constants a, b, and c are defined as

$$a = 6\left[\frac{(1-\gamma_1^2)}{E_1 t_1^2} - \frac{(1-\gamma_2^2)}{E_2 t_2^2}\right], \tag{31}$$

$$b = 12\left[\frac{(1-\gamma_1^2)}{E_1 t_1^3} + \frac{(1-\gamma_2^2)}{E_2 t_2^3}\right], \tag{32}$$

$$c = 4\left[\frac{(1-\gamma_1^2)}{E_1 t_1} + \frac{(1-\gamma_2^2)}{E_2 t_2}\right]. \tag{33}$$

The solution of Eq. (30) is related to the roots of the algebraic equation

$$y^3 - \frac{G_0 c}{\eta} y^2 + \frac{E_0 b}{\eta} y - \frac{G_0 E_0 (bc - a^2)}{\eta^2} = 0.$$

It can be shown that the roots to the above equation always contain one pair of complex conjugates and one positive real root. In other words the solution must be in the form

$$\begin{aligned}\sigma_0 = {} & A_1 \cosh \beta_1 x + A_2 \sinh \beta_1 x + A_3 \cosh \beta_H x \cos \beta_V x \\ & + A_4 \sinh \beta_H x \cos \beta_V x \\ & + A_5 \sinh \beta_H x \sin \beta_V x + A_6 \cosh \beta_H x \sin \beta_V x.\end{aligned} \tag{34}$$

In general, there are six boundary conditions from which to determine A_1 to A_6. But symmetry about the plane $x = 0$ would reduce the solution to

$$\begin{aligned}\sigma_0 = {} & A_1 \cosh \beta_1 x + A_3 \cosh \beta_H x \cos \beta_V x \\ & + A_5 \sinh \beta_H x \sin \beta_V x.\end{aligned} \tag{35}$$

The constants A_1, A_3, and A_5 are completely determined by the boundary conditions that at the edge $x = \ell$, moments, horizontal forces, and shear forces vanish. Also the shear stress is given by

$$\begin{aligned}\tau_0 = {} & C_1 \sinh \beta_1 x + C_2 \sinh \beta_H x \cos \beta_V x \\ & + C_3 \cosh \beta_H x \sin \beta_V x.\end{aligned} \tag{36}$$

Details of expressions for A_1, A_3, A_5, and C_1, C_3, C_5 are given in Appendix B.

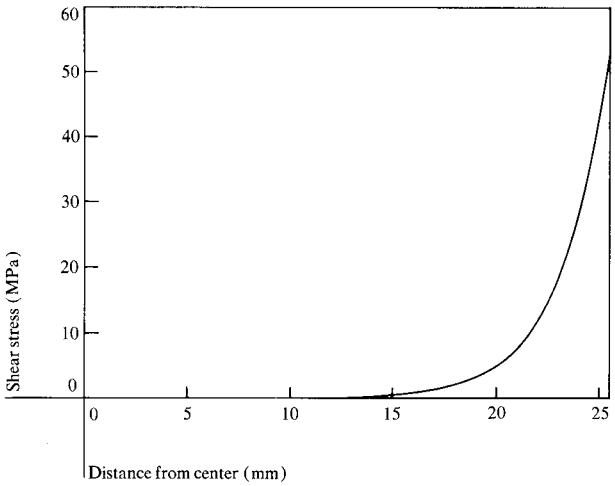

Figure 4 Shear stress distribution over width of joint.

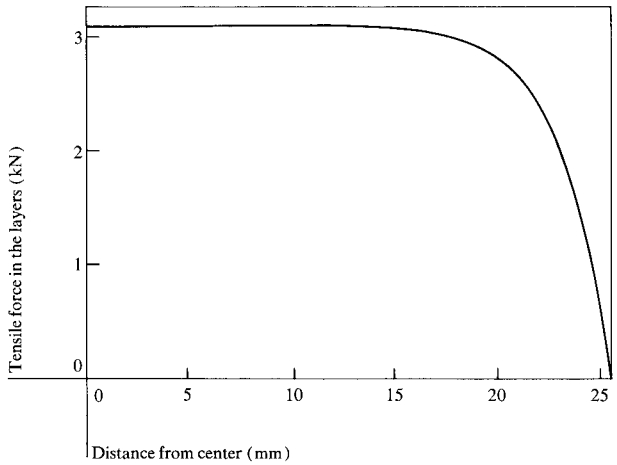

Figure 5 Force induced by thermal expansion.

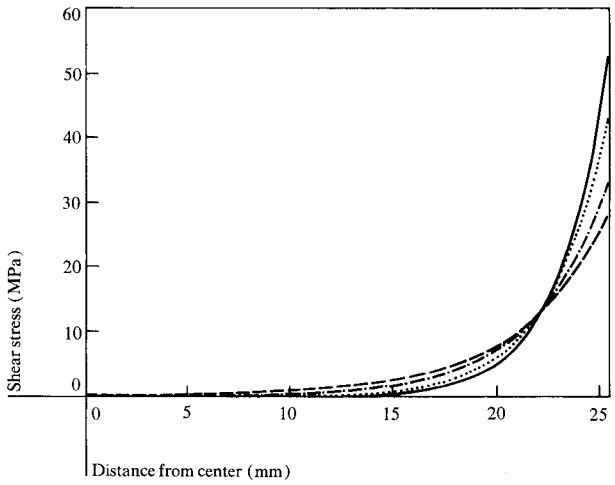

Figure 6 Shear stress distribution over width of joint for four joint thicknesses.

Numerical examples and discussion

Two layers without bending

Numerical examples are shown for the following material and geometrical parameters for a 100°C rise in temperature:

Young's modulus E	1.17×10^{11} Pa	2.75×10^{11} Pa
Thickness t	1.57 mm	1.52 mm
Thickness exp. coef.	1.6×10^{-5}/°C	6.5×10^{-6}/°C
Shear modulus of joint material		1.23×10^{9} Pa
Joint thickness		0.051 mm
Joint width		51 mm

Figure 4 shows the shear stress distribution in the joint. As may be expected, the maximum shear stress occurs at the edge and is found to be 5.3×10^7 Pa. The associated shear strain is 0.043. Often one assumes the shear modulus of the joint material to be very soft compared to the joined material; and the strain and stress calculated under that assumption are 0.475 and 5.85×10^8 Pa, more than ten times larger than the elastic solution. Also, Eq. (15) gives a very accurate estimate (0.5% low) of the actual shear stress. Figure 5 shows the tensile force in the layer and how it drops to zero near the edge of the joint. This calculation illustrates that, in this situation, about 60% of the joint material in the center is not really structurally effective. Only the section from 15 mm outward is effectively stressed.

Figure 6 shows the different maximum shear stresses where the joint thicknesses are taken to be 0.051, 0.076, 0.127, and 0.178 mm. It illustrates that while the thickness may change from 0.051 mm to 0.178 mm, an increase of 3.5 times, the shear stress decreases by a factor of 1.8 only. While this may be expected from examination of Eqs. (13), (14), and (15), it is not immediately obvious from intuition.

Three layers without bending

It is difficult to draw any general conclusion from the three-layer case because so many physical parameters, thicknesses, expansion coefficients, and elastic moduli could all be varying. Consider the previous case of two layers illustrated in Figs. 4 and 5. Let us put another layer of material in between with modulus $E = 2.62 \times 10^{11}$ Pa and thickness 0.51 mm. The other joint thickness and modulus remain the same as before. The thermal expansion coefficient is taken as 3×10^{-6}/°C, less than the other two coefficients. The shear stress distributions are shown

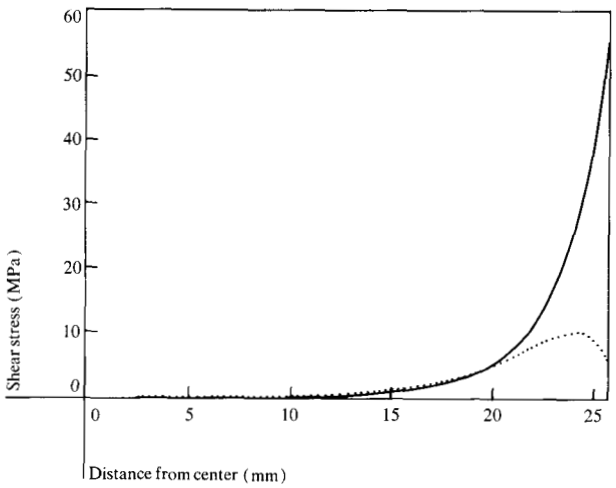

Figure 7 Shear stress distributions over width of joints.

in Fig. 7. The solid line may be compared to Fig. 4, showing that there is a slight increase in maximum shear stress. The dotted line shows the shear stress distribution in the joint between the two materials with expansion coefficients 3.0×10^{-6} and 6.5×10^{-6}. The maximum stress is not at the edge. This example illustrates that when there are three layers, simple physical intuitive ideas may be useful but not always applicable.

Two layers allowing free flexure

For illustrative purposes numerical results are presented for the case of different layers allowing free flexure for the same material properties used in the previous two-layer case without bending.

Figures 8 and 9 show the tensile and shear stress distributions in plane strain for two different thicknesses. The joint material is given by $E = 3.45 \times 10^9$, $G = 1.23 \times 10^9$ Pa. Note that the thicker joint produces the lower stress. Particularly of note is the characteristic that the stresses remain almost zero for most of the joint length, except in the vicinity of the edge, where the stress rises dramatically. Also, the tensile stress changes from negative to positive a small distance in from the edge; but the shear stress does not change sign. This is a common characteristic of this problem. Finally, it is noteworthy that the maximum shear stresses for the two cases are 4×10^7 and 2.56×10^7 Pa, respectively. The corresponding shear stresses for plane stress are 2.75×10^7 and 1.75×10^7 Pa, respectively. A simple stress estimate by using differential thermal expansion divided by joint thickness would give a gross overestimate of 5.85×10^8 and 2.34×10^8 Pa, respectively.

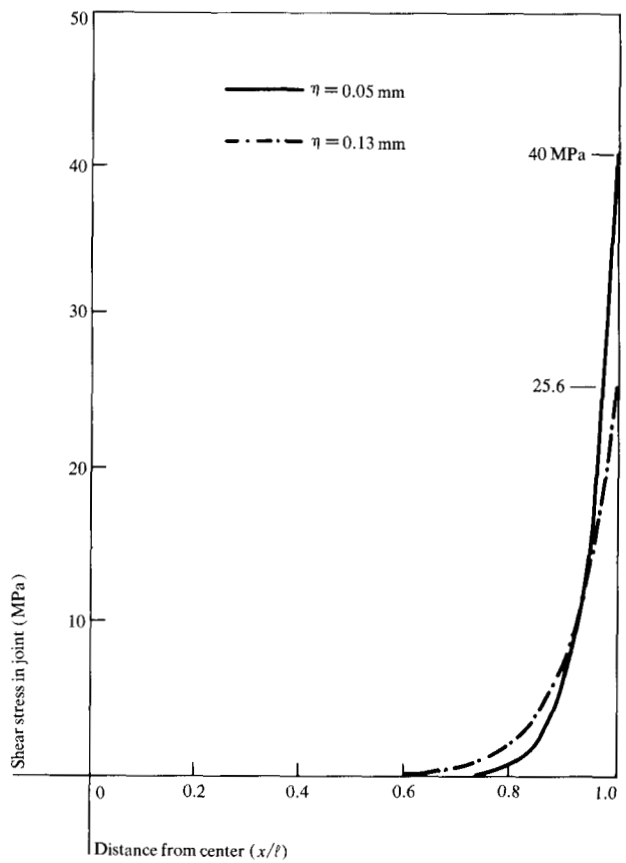

Figure 8 Shear stress distribution in joint with flexure.

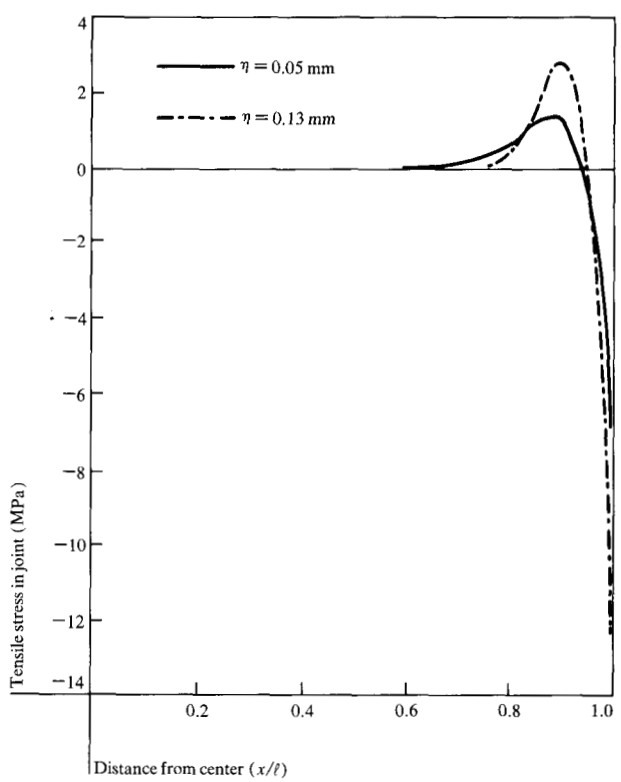

Figure 9 Tensile stress distribution in joint with flexure.

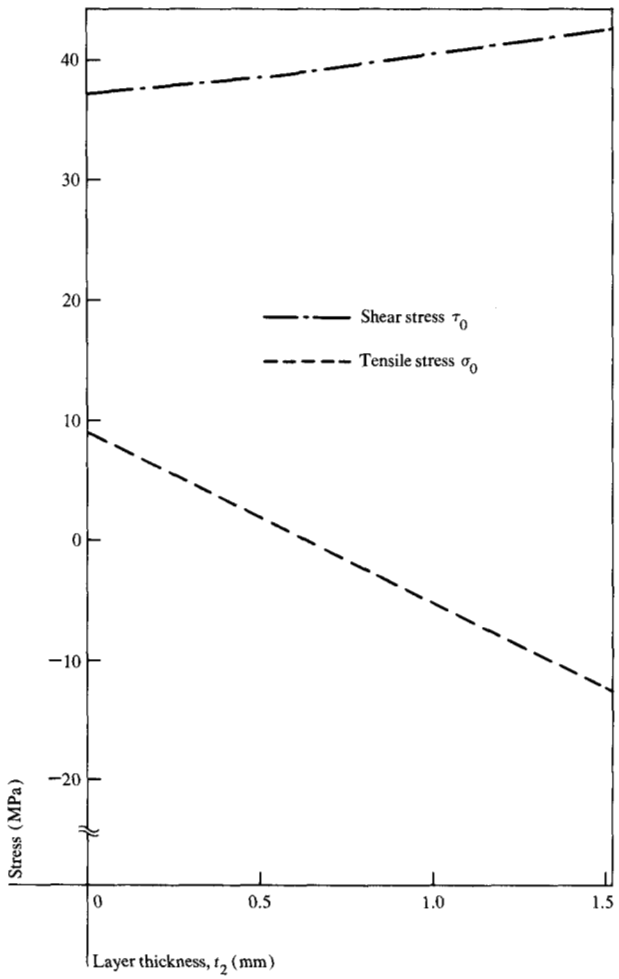

Figure 10 Effect of variation of layer thickness t_2.

Figure 10 shows the effects of varying the thickness of layer 2 from 0.76 to 1.52 mm. The tensile stress at the free edge changes from positive to negative, while the shear stress increases slightly. If the joint material is weak in tension, a condition often referred to as peel stress, keeping this stress component negative may be desirable.

The maximum shear stress computed from Eq. (14) turns out to be almost one half the value for this case (plane stress). This has been found characteristically so for a number of other cases. It is concluded that free bending relaxes shear stresses at the edge.

A calculation for the forces and moments in the two layers in these numerical examples checks with the results given by Timoshenko's well-known bimetallic thermostat solution. This indicates that for the physical parameters used in this paper the numerical results for forces and moments agree with this analysis extremely well. In other words, if one is only interested in moment and deflection but not the joint stresses, Timoshenko's analysis is still applicable.

Summary

This paper provides some insight and tools to understand the stress distribution in a bonded joint induced by thermal expansion of dissimilar materials. The maximum shear stress always occurs at the edge of the joint. When flexure is allowed, significant tensile stress may occur. However, the flexure does decrease the maximum shear stress.

It is difficult to draw conclusions from the three-layer case, since many more physical parameter variables are possible. The analysis still indicates that the maximum shear stress in either of the two joints usually occurs at the edges, and that there is an interaction from one joint to another if the middle layer is reasonably thin.

Appendix A: Analysis of two bonded circular sheets

The physical parameters and geometrical dimensions are shown in Fig. 3. The polar coordinates (r, θ) are employed. The stress-strain-temperature relationships of layers 1 and 2 are

$$e_r^{(i)} = \frac{du_i}{dr} = \frac{\sigma_r^{(i)} - \gamma_i \sigma_\theta^{(i)}}{E_i} + T\alpha_i \qquad (i = 1, 2). \tag{A1}$$

The assumption of uniform shear stress through the thickness of the joint gives the relationship

$$\frac{\tau}{G} = \frac{u_1 - u_2}{\eta}. \tag{A2}$$

The equilibrium conditions in each sheet give

$$\left(\sigma_r^{(1)} - \sigma_\theta^{(1)} + r\frac{d\sigma_r^{(1)}}{dr}\right) t_1 = \tau r,$$

and

$$\left(\sigma_r^{(2)} - \sigma_\theta^{(2)} + r\frac{d\sigma_r^{(2)}}{dr}\right) t_2 = -\tau r. \tag{A3}$$

The thermal stress problem is formulated by Eqs. (A1) to (A3) with the proper boundary conditions. The general solution for the shear stress to the above equations is found in terms of the modified Bessel functions,

$$\tau = A[I_1(\beta r) + BK_1(\beta r)], \tag{A4}$$

where A and B are constants, and

$$\beta^2 = \frac{G}{\eta}\left(\frac{1 - \gamma_1^2}{E_1 t_1} + \frac{1 - \gamma_2^2}{E_2 t_2}\right). \tag{A5}$$

The stresses and displacements in layer 1 are given by

$$(\sigma_\theta^{(1)} + \sigma_r^{(1)})t_1 = \frac{A(1 + \gamma_1)}{\beta}[I_0(\beta r) + BK_0(\beta r) + C_1], \tag{A6}$$

$$u_1 - \alpha_1 Tr = \frac{(1-\gamma_1^2)}{E_1 t_1 \beta^2}\left[I_1(\beta r) + BK_1(\beta r) + \frac{\beta C_1 r}{2} + \frac{D_1}{r}\right]. \tag{A7}$$

The expressions for corresponding quantities for layer 2 may be found by changing the corresponding indices from 1 to 2 and adding a negative sign to one side of each equation. The constants C_1, C_2, D_1, and D_2 are related by the equations

$$D_1 + D_2 = 0, \tag{A8}$$

$$A(C_1 + C_2) = -\frac{2(\alpha_1 - \alpha_2)TG}{\eta\beta}. \tag{A9}$$

There are four boundary conditions, which, together with the above two, are sufficient to solve for all six constants.

In the case of a solid disk with radius R, three of the six constants are zero:

$$B = D_1 = D_2 = 0. \tag{A10}$$

The condition that at radius R the radial stress components are zero leads to

$$C_1 = \frac{2}{1+\gamma_1}\left[\frac{1-\gamma_1}{\beta R} I_1(\beta R) - I_0(\beta R)\right], \tag{A11}$$

$$C_2 = \frac{2}{1+\gamma_2}\left[\frac{1-\gamma_2}{\beta R} I_1(\beta R) - I_0(\beta R)\right]. \tag{A12}$$

The shear stress is given by

$$\tau = -\frac{2(\alpha_1 - \alpha_2)TG}{(C_1 + C_2)\eta\beta} I_1(\beta r).$$

From the properties of modified Bessel function I_n, it is clear that the shear stress reaches a maximum at the outer edge and is zero at the center.

Appendix B

In the main text it has been explained that the six roots of the characteristics of Eq. (30) can be written in the forms

$$\beta_1, -\beta_1, \beta_H + i\beta_V, \beta_H - i\beta_V, -\beta_H + i\beta_V, -\beta_H - i\beta_V.$$

The three constants A_1, A_2, and A_3 are determined from the following set of algebraic equations:

$$\begin{aligned}
&\beta_1^2 \cosh \beta_1 \ell A_1 \\
&\quad + [(\beta_H^2 - \beta_V^2)\cosh \beta_H \ell \cos \beta_V \ell \\
&\quad - 2\beta_H\beta_V \sinh \beta_H \ell \sin \beta_V \ell]A_3 \\
&\quad + [(\beta_H^2 - B_V^2)\sinh \beta_H \ell \sin \beta_V \ell \\
&\quad + 2\beta_H\beta_V \cosh \beta_H \ell \cos \beta_V \ell]A_5 = 0,
\end{aligned} \tag{B1}$$

$$\begin{aligned}
&\frac{\sinh \beta_1 \ell}{\beta_1} A_1 + \left[\frac{\beta_V}{(\beta_H^2 + \beta_V^2)}\cosh \beta_H \ell \sin \beta_V \ell \right. \\
&\qquad \left. + \frac{\beta_H}{(\beta_H^2 + \beta_V^2)}\sinh \beta_H \ell \cos \beta_V \ell\right] A_3 \\
&\qquad + \left[\frac{\beta_H}{(\beta_H^2 + \beta_V^2)}\cosh \beta_H \ell \sin \beta_V \ell \right. \\
&\qquad \left. - \frac{\beta_V}{(\beta_H^2 + \beta_V^2)}\sinh \beta_H \ell \cos \beta_V \ell\right] A_5 = 0,
\end{aligned} \tag{B2}$$

$$\begin{aligned}
&\left[\left(\beta_1^4 + \frac{E_0 b}{\eta}\right)\cosh \beta_1 \ell\right] A_1 \\
&\quad + \left\{\left[(\beta_H^2 - \beta_V^2) - 4\beta_H^2\beta_V^2 + \frac{E_0 b}{\eta}\right]\cosh \beta_H \ell \cos \beta_V \ell \right. \\
&\qquad \left. - 4\beta_H\beta_V(\beta_H^2 - \beta_V^2)\sinh \beta_H \ell \sin \beta_V \ell\right\} A_3 \\
&\quad + \left\{\left[(\beta_H^2 - \beta_V^2)^2 - 4\beta_H^2\beta_V^2 + \frac{E_0 b}{\eta}\right]\sinh \beta_H \ell \sin \beta_V \ell \right. \\
&\qquad \left. + 4\beta_H\beta_V(\beta_H^2 - \beta_V^2)\cosh \beta_H \ell \cos \beta_V \ell\right\} A_5 \\
&= \left(\frac{E_0 b}{\eta}\right)\left(\frac{G_0 C}{\eta}\right)\left(\frac{9}{bc}\right)[(1+\gamma_1)\alpha_1 - (1+\gamma_2)\alpha_2]T,
\end{aligned} \tag{B3}$$

$$C_1 = \frac{1}{\beta_1}\left(\frac{\eta}{E_0 b}\right)\left(\frac{b}{a}\right)\left(\beta_1^4 + \frac{E_0 b}{\eta}\right) A_1, \tag{B4}$$

$$C_2 = \left(\frac{\eta}{E_0 b}\right)\left(\frac{b}{a}\right)[\gamma_1 A_3 - \gamma_2 A_5], \tag{B5}$$

$$C_3 = \left(\frac{\eta}{E_0 b}\right)\left(\frac{b}{a}\right)[\gamma_1 A_5 + \gamma_2 A_3], \tag{B6}$$

$$\gamma_1 = \beta_H\left[\frac{E_0 b}{\eta(\beta_H^2 + \beta_V^2)} + \beta_H^2 - 3\beta_V^2\right], \tag{B7}$$

$$\gamma_2 = \beta_V\left[\frac{E_0 b}{\eta(\beta_H^2 + \beta_V^2)} + \beta_V^2 - 3\beta_H^2\right]. \tag{B8}$$

References

1. *Physical Design of Electronic Systems*, Vol. II, *Materials—Technology*, Vol. III, *Integrated Device and Connection Technology*, prepared by staff of Bell Telephone Lab., Inc., Prentice-Hall, Inc., Englewood Cliffs, NJ, 1971.
2. *Reliability of Semiconductor Devices, Proc. IEEE* **62,** No. 2, 1974.
3. E. Klokholm and B. S. Berry, "Intrinsic Stress in Evaporated Metal Films," *J. Electrochem. Soc.* **115,** 823–826 (1968).
4. T. C. Taylor and F. L. Yuan, "Thermal Stress and Fracture in Shear Constrained Semiconductor Structure," *IRE Trans. Electron. Devices* **ED9,** 303–308, (1963).
5. O. Volkersen, *Luftfahrtforschung* **15,** 41 (1938).
6. M. Goland and E. Reissner, "The Stresses in Cemented Joints," *J. Appl. Mech., Trans. ASME* **11,** 17–27 (1944).
7. N. K. Benson, "The Mechanics of Adhesive Bonding," *Appl. Mech. Rev.*, February 1961.
8. D. D. Eley, ed., *Adhesion—Fundamentals & Practice*, Maclaren & Sons, London, 1969.

9. D. Satas, ed., *Conference on Adhesion of Polymers*, Wayne State University, Detroit, MI, 1967.
10. R. Houwink and G. Salomon, eds., *Adhesion & Adhesives*, Vols. I and II, 2nd revised edition, Elsevier, Amsterdam, 1967.
11. R. Patric, ed., *Treatise on Adhesion & Adhesives*, Vols. 1 and 2, Marcel Dekker, New York, 1968.
12. Lieng-Huang Lee, *Recent Advances in Adhesion*, Palmerton, New York, 1976.
13. L. M. Keer and K. Chantaramungkorn, "Stress Analysis for a Double Lap Joint," *Trans. ASME, Series E, J. Appl. Mech.* **42,** 353 (1975).
14. W. J. Renton and J. R. Vinson, "Analysis of Adhesively Bonded Joints between Panels of Composite Materials," *Trans. ASME, Series E, J. Appl. Mech.* **44,** 101-106 (1977).
15. G. J. Spies, *J. Aircraft Engr.* **25,** 64 (1953).
16. J. J. Bikerman, *J. Appl. Phys.* **28,** 1484 (1957).
17. J. J. Bikerman, *The Science of Adhesive Joints*, Academic Press, Inc., New York, 1961.
18. D. H. Kaelble, "Theory and Analysis of Peel Adhesion; Bond Stresses and Distribution," *Trans. Soc. Rheology* **IV,** 45-73 (1960).
19. D. H. Kaelble, *Physical Chemistry of Adhesions*, John Wiley & Sons, Inc., New York, 1971.
20. S. Timoshenko, "Analysis of Bi-metal Thermostats," *J. Opt. Soc. Amer.* **11,** 233-255 (1925).

Received November 1, 1977; revised September 7, 1978

W. T. Chen is located at the IBM System Products Division laboratory, P.O. Box 6, Endicott, New York 13760, and C. W. Nelson, who is retired, is at 610 Bassett Avenue, Endicott, New York 13760.